Multidimensional coupled sedimentation and consolidation theory

Murray Fredlund, Jim Zhang
SoilVision Ltd., Saskatoon, Saskatchewan, Canada

Dirk van Zyl
University of British Columbia, Vancouver, British of Columbia, Canada

Sean Wells
Suncor Inc., Calgary, Alberta, Canada

ABSTRACT: Modelling of the sedimentation and consolidation processes requires specialized software and unified theories. This paper discusses the numerical modeling of coupled sedimentation and large strain consolidation. Using the two-phase flow theory, it is possible to unify the theories of sedimentation and consolidation with consistent variables and coordinates, and the one-dimensional unified governing equation can be extended to a three-dimensional formulation. Four benchmarks were evaluated. These benchmarks included the Sidere Benchmark, originally derived by Bartholomeeusen et al. and the Townsend benchmarks for scenario A, B, and D. Townsend A was solved as a 2D and 3D column to show that the multidimensional formulation demonstrates consistent results.

1 INTRODUCTION

Oil sands tailings sedimentation and consolidation may take very long times. For example, the field data measured in Suncor Pond 1A (Wells 2011) shows that average solids content is increased only about 5.1% in 28 years from the average value of 30.8% in 1982 to 35.9% in 2010. Therefore, numerical models which represent the process of tailings sedimentation, dewatering, and consolidation is of importance to model the long-term management of tailings facilities.

Consolidation theories have been utilized in Geotechnical engineering for many years. The disposal of tailings slurry has forced a realization that there is a point at which void ratios are high and the material behavior is governed by sedimentation rather than consolidation theory. This paper presents the coupling of sedimentation theory with large strain consolidation theories for the purpose of modeling tailings slurries. SVFlux has been historically used to solve seepage problems for unsaturated or saturated soils, while SVSolid can be used to analyse soil strength-deformation. The coupling of SVFlux and SVSolid can be utilized to solve sedimentation and consolidation problems including small strain and large strain consolidation.

This paper outlines the theory behind the implementation of the coupled sedimentation and consolidation processes.

2 SEDIMENTATION AND CONSOLIDATIN PROCESS

The major theories of sedimentation and consolidation were developed independently in different areas (Toorman, 1996; O'Neil, 2002). Sedimentation theory is primarily utilized in the field of chemistry, while consolidation theory (Terzaghi 1943, Biot 1941) is primarily used in soil mechanics. Subsequent research was able to link the two to develop a unified theory of sedimentation and consolidation.

Been (1980) was the first to show the similarity between Kynch's theory and the traditional consolidation. It is found that both the Kynch sedimentation equation and the general large strain equation developed by Gibson et al (1967) can be derived from the two phase flow model. Been (1980, 1981) also noticed that the effective stress is zero in the sedimentation process of suspension. Pane and Schiffman (1985) introduced an interaction coefficient to describe the effective stress changing transition from sedimentation to consolidation. Another formulation of large strain consolidation proposed by Somogyi (1980) is expressed as the variable of excess pore water pressure in the governing equation. Jeeravipoolvarn (2010) used the Somogyi's equation and Pane's interaction coefficient to model sedimentation and consolidation in the oil sands tailings. The development to link the sedimentation and consolidation was also presented by Li and Mehta (1998), Toorman (1996, 1999), and Karl and Wells (1999).

2.1 Kynch sedimentation theory

Kynch (1952) proposed a theory of sedimentation which has become popular. It is assumed that at any point in the suspension the velocity of falling particle depends only on the local concentration of particles. Kynch introduced a concept of particle flux. The governing equation of sedimentation for the suspension of particles was obtained according to the mass conservation, i.e.

$$\frac{\partial \phi}{\partial t} + \frac{\partial (f_{bk}(\phi))}{\partial y} = 0 \tag{1}$$

If the Kynch settling velocity is constant, then equation (1) can be rewritten as:

$$\frac{\partial \phi}{\partial t} + v_s \frac{\partial (\phi)}{\partial y} = 0 \tag{2}$$

where ϕ is the volumetric solids fraction; $f_{bk}(\phi)$ is mass flux; and v_s is the solid settling velocity.

2.2 Choice of variable

The state of sedimentation in a suspension can be described using different variables. The most commonly used variables include void ratio e (Gibson et al.1967), porosity n (Lee 1979), volume solid fraction ϕ (Toorman, 1996), excess pore water pressure u_e (Somogyi 1984, Jeeravipoolvarn 2010), and concentration C.

One problem in using void ratio as the primary variable is that it tends to an infinite value when the mass fraction of a suspension is zero. The parameter of volume fraction has no such problem, but the value of $\phi = 1$ never occurs in practice (Toorman, 1999). The porosity has the a similar limitation.

2.3 Coordinate system and transformation

There are two types of coordinate systems: Eulerian and Lagrangian. The Eulerian space is global and external, and Lagrangian space is local and interior. The governing equation can be formulated in Eulerian coordinate system or in Lagrangian system. To implement the numerical model with the formulation of Eulerian system, the moving mesh scheme must be adopted for the large-strain deformation. However, the numerical calculation can be realized under a fixed coordinate if the governing equation is formulated in the Lagrangian coordinate system. The relationship between the Eulerian and Lagrangian coordinate can be expressed as

$$\xi = X + u + u_0, \quad \zeta = Y + v + v_0, \quad \eta = Z + w + w_0 \tag{3}$$

where ξ, ζ, and η are the Eulerian coordinate; X, Y, and Z are Lagrangian coordinate; u, v, and w are the displacement of soil solids; and u_0, v_0, w_0 are the initial displacement of solids.

Any function $F(\xi, \zeta, \eta)$ formulating in the Eulerain space can be represented in the Langrangian space with a general coordinate transformation. However, the equation (4) is a simplified coordinate transformation for use in the 1D or quasi-2D/3D model.
.

$$\frac{\partial F(\xi,\zeta,\eta)}{\partial \eta} = \frac{1+e_0}{1+e} \frac{\partial F(\xi,\zeta,\eta)}{\partial Z} \tag{4}$$

2.4 3D governing equation in Eulerian space

Most available models for sedimentation and consolidation can be developed according to a two-phase flow model, which is based on the following assumption (Gibson, English, & Hussey, 1967), (Gibson, Schiffman, & Cargill, 1981), (Lee, 1979), (Tan, 1985), (McVay & Bloomquist, 1986), (McVay, Zuloaga, & Townsend, 1988), (Burger & Wendland, 2001), and (Gustavsson, 2003):

- The mixture is saturated and is composed of fluid and a solid phase,
- The solid and fluid phase themselves are incompressible,
- No mass transfer takes place between the two phases,
- Surface tension between the phases is neglected,
- The relative velocity between the soil matrix and the pore fluid is governed by the Darcy-Gersevanov equation,
- Soil compressibility and permeability are uniquely determined by the state parameter of the mixture, such as void ratio, or volume fraction.

With above assumptions the governing equation for water flow can be obtained with the formulation of Eulerian space:

$$\frac{\partial}{\partial \xi}\left[\frac{k_\xi}{\gamma_w}\frac{\partial(u_e)}{\partial \xi}\right] + \frac{\partial}{\partial \zeta}\left[\frac{k_\zeta}{\gamma_w}\frac{\partial(u_e)}{\partial \zeta}\right] + \frac{\partial}{\partial \eta}\left[\frac{k_\eta}{\gamma_w}\frac{\partial(u_e)}{\partial \eta}\right] = \frac{1}{1+e}\left[\frac{D[\theta_w(1+e)]}{Dt}\right] \tag{5}$$

where k_ξ, k_ζ, and k_η are the hydraulic conductivity along ξ, ζ, and η direction; u_e is the excess pore water pressure; $D[\theta_W(1 + e)]/Dt$ is the material derivation, which can be extended to

$$\frac{D[\theta_w(1+e)]}{Dt} = \frac{\partial[\theta_w(1+e)]}{\partial t} + v_{s\xi}\frac{\partial[\theta_w(1+e)]}{\partial \xi} + v_{s\zeta}\frac{\partial[\theta_w(1+e)]}{\partial \zeta} + v_{s\eta}\frac{\partial[\theta_w(1+e)]}{\partial \eta} \tag{6}$$

where $v_{s\xi}$, $v_{s\zeta}$ and $v_{s\eta}$ are the solids settling velocity in ξ, ζ, and η direction.

2.5 3D governing equation in Lagrangian scheme

Using the equation (4) as the coordinate transformation, the governing equation (5) can be formulated in the Lagrangrian coordinate. This paper will focus on the saturated soil, so that the Terzaghi's effective stress principle will be applied in the following derivation of stress equilibrium, and governing equation for 1D or quasi-2D/3D.

2.5.1 Stress equilibrium:

If the shear strength in xz and yz plane can be neglected in the modeling of tailings consolidation and sedimentation, the stress equilibrium equation in Lagrangian scheme could be expressed as the equation (7) for the saturated soil:

$$\frac{\partial \sigma_z}{\partial Z} + \gamma_w\frac{\partial w}{\partial Z} + \frac{\gamma_s - \gamma_w}{1+e_0} = 0 \tag{7}$$

where γ_s and γ_w is the unit weight of solids and water respectively.

2.5.2 Quasi-2D/3D governing equation:

Quasi-2D/3D means the water can flow in true 2D or 3D space, but the solid deformation is limited to occur in the vertical direction (Jeeravipoolvarn 2010). Considering the strain $\varepsilon_x = 0$ and $\varepsilon_y = 0$, and using coordinate transformation (4), the governing equation (5) can be represented as the equation (8) that is similar to the formulation obtained by Jeeravipoolvarn (2010):

$$\frac{1+e}{1+e_0}\left[\frac{\partial}{\partial X}\left(\frac{k_X}{\gamma_w}\frac{\partial u_e}{\partial X}\right)+\frac{\partial}{\partial y}\left(\frac{k_Y}{\gamma_w}\frac{\partial u_e}{\partial Y}\right)\right]+\frac{\partial}{\partial z}\left[\frac{k_Z}{\gamma_w}\frac{1+e_0}{1+e}\frac{\partial u_e}{\partial Z}\right]+$$

$$v_s\left[\frac{\theta_w}{a_v(1+e)}\left(\frac{(\gamma_s-\gamma_w)}{1+e_0}+\frac{\partial u_e}{\partial Z}\right)-\frac{\partial\theta_w}{\partial Z}\right]-\frac{\theta_w}{(1+e_0)a_v}\left[(\gamma_s-\gamma_w)FR+\frac{\partial q(t)}{\partial t}\right] \tag{8}$$

$$=\frac{(1+e)}{1+e_0}\frac{\partial\theta_w}{\partial t}-\frac{\theta_w}{a_v(1+e_0)}\frac{\partial u_e}{\partial t}$$

$$FR=\frac{\partial(\Delta Z)}{\partial t}\Big/(1+e_0),\quad a_v=\frac{\partial\sigma'}{\partial e} \tag{9}$$

where FR is the solid filling rate; $\partial(\Delta Z)/\partial t$ is the tailing mixture filling rate; $\partial(q(t))/\partial t$ is the surcharge rate; v_s is the solid settling velocity; and σ' is the effective stress.

2.5.3 *Somogyi equation:*
In 1D case the equation (8) is further reduced to the similar formulation to the Somogyi equation (Somogyi 1984):

$$\frac{\partial}{\partial z}\left[\frac{k_Z}{\gamma_w}\frac{1+e_0}{1+e}\frac{\partial u_e}{\partial Z}\right]+v_s\left[\frac{\theta_w}{a_v(1+e)}\left(\frac{(\gamma_s-\gamma_w)}{1+e_0}+\frac{\partial u_e}{\partial Z}\right)-\frac{\partial\theta_w}{\partial Z}\right]$$

$$-\frac{\theta_w}{(1+e_0)a_v}\left[(\gamma_s-\gamma_w)FR+\frac{\partial q(t)}{\partial t}\right]=\frac{(1+e)}{1+e_0}\frac{\partial\theta_w}{\partial t}-\frac{\theta_w}{a_v(1+e_0)}\frac{\partial u_e}{\partial t} \tag{10}$$

2.5.4 *Hindering settling rate:*
As required in equation (8) and (10), the sedimentation process is included through the solid settling velocity, v_s, which mainly occurs when the effective stress is less than a minimum value σ'_{min}, or void ratio is larger than a critical value e_m. Many experiments for oil sands tailings material show that when $\sigma'_{mim} < 0.1$ kPa, there is no unique relationship between the effective stress and void ratio, implying that no steady soil structure is formed. Therefore, the value of $\sigma'_{min} = 0.1$ kPa could be chosen, and e_m can be determined by the material compressibility curve at the given σ'_{min}.

For the stability consideration in the numerical calculation, the settling velocity can be expressed as a smooth function related to the Stokes velocity and solids content or porosity (Pane & Schiffman 1997):

$$v_s=v_{st}f(n) \tag{11}$$

where v_{st} is the Stokes velocity for particle settling; $f(n)$ is a function related to the soil porosity.
Richardson and Zaki (1954) proposed an empirical expression as follows:

$$v_s=v_{st}(1-\phi_s)^\alpha \tag{12}$$

where ϕ_s is volumetric solid content; and α is an empirical parameter verifying in the range 5 to 30 for silty natural material (McRobert & Nixon 1976).

Toorman (1996) and Pane & Schiffman (1997) presented a relationship between particles settling veolocity and hydraulic conductivity, as given in equation (13):

$$v_s=\left(\frac{\gamma_w}{\gamma_s}-1\right)\frac{k}{1+e} \tag{13}$$

where k is the hydraulic conductivity.

3 BENCHMARKING

The governing equations (8) and (10) were implemented in the SVOffice package by coupling the SVSolid and SVFlux software. Equation (10) is verified with the Sidere benchmark (Bartholomeeusen 2002) and Townsend benchmarks (Townsend 1990). The quasi-2D/3D equation (8) is verified by comparison of results simulated with the 1D/2D/3D software for Townsand A scenario.

3.1 *1D –Sidere benchmarking (Bartholomeeusen 2002)*

Bartholomeeusen (2002) presented a benchmark referenced as Sidere for 1D large strain consolidation. In Sidere benchmark the experimental results were available to compare the pond height, and density profiles, and excess pore pressure. The purpose of this benchmark is to verify the correct implementation of the Somogyi equation in the software.

3.1.1 *Model description:*
The model domain is a 1D column with the parameters of initial height = 0.565 *m*, initial density = 1495 kg/m^3, and initial void ratio = 2.47 with a specific gravity = 2.72. A stable soil structure is formed initially. Only self-weight consolidation is considered in the Sidere benchmark.

The upper boundary of the model is freely drained, i.e., satisfying excess pore pressure, u_e = 0. The bottom of the model is impermeable for water flow. The material compressibility and permeability obeys the power function, as given in the equation (13) and (14):

$$e = A\left(\sigma' + Z_c\right)^B \tag{13}$$

$$k = Ce^D \tag{14}$$

where *A*, *B*, *C*, and *D* are experimental parameters. The value of these parameters are *A* = 1.69 *kPa*, *B* = -0.12, Z_c =0.046, *C* = 4.14E-9 *m/s*, and *D* = 6.59.

3.1.2 *Model results:*
The model is setup to simulate 7 days. Figure 1a is the simulated pond height comparing with the experimental data. The legend "SVSomogyi – 1DLC" in figure 1a stands for the Somogyi model for the large strain consolidation implemented in the SVOffice software. For comparison figure 1b illustrated the pond height predicted by other authors in Sidere benchmark. The comparison of mixture density with experimental data is presented in figure 2, where figure 2a is the results simulated in this paper, and figure 2b is the results by other authors. The experimental data is fluctuated, because it was recorded by X-ray.

It can been seen from the figure 1 and 2 that the predicted pond height and density does not well match the experimental data with the material properties as given in the benchmarking. However, by comparison with results obtained by other authors, the values simulated in this paper are pretty close to the experimental data.
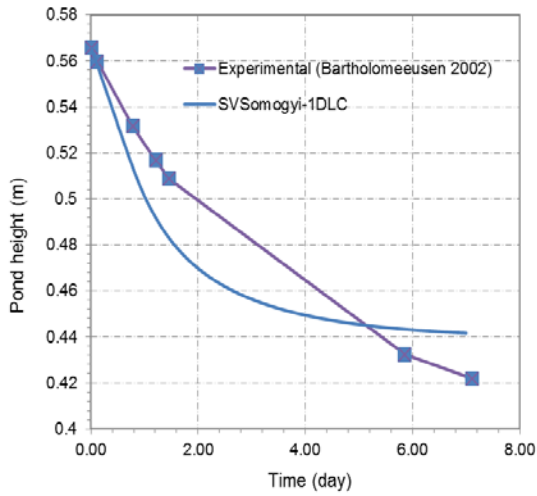
Figure 1a. Comparison of predicted pond height with experimental data for Sidere benchmarking
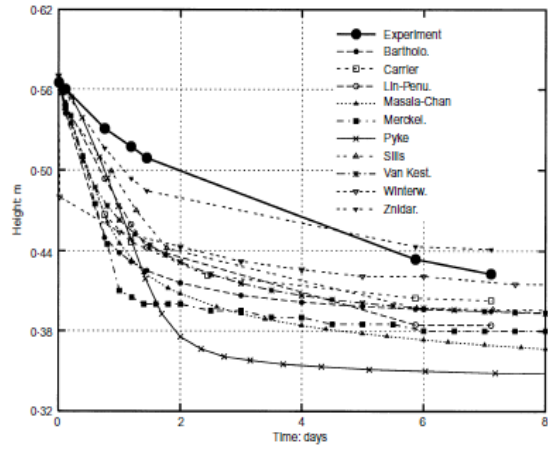
Figure 1b. Pond height predicted by other authors for Sidere benchmarking (after Bartholomeeusen 2002)
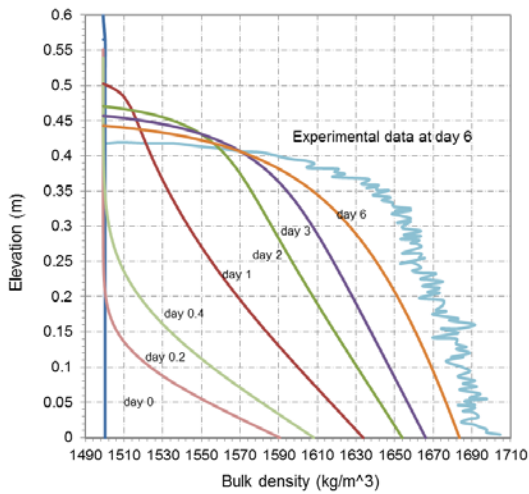

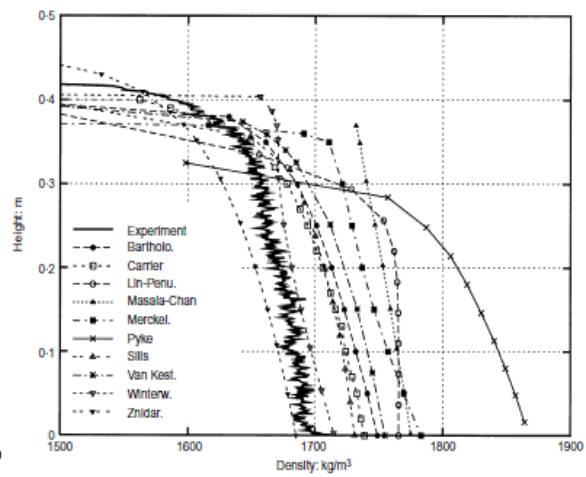Figure 2a. Profiles of the predicted mixture density for Sidere benchmarking

Figure 2b. Profiles of the mixture density predicted by other authors for Sidere benchmarking (after Bartholomeeusen 2002)

3.2 *Townsend benchmarks*

Townsend & McVay (1990) presented 4 scenarios to predict large strain consolidation. These examples are commonly recognized as the most popular benchmark for the evaluation of nu-

merical model analysis of large strain consolidation. Scenario A is designed for the simulation of quiescent consolidation with a uniform initial solids content = 16%, scenario B is continuous filling, scenario C is quiescent consolidation with a constant surcharge, and scenario D is two layers of quiescent consolidation with the sand/clay capped and non-uniform initial solids content. This paper presents the comparison with the scenario A, B, and D.

3.2.1 Model description for Townsend scenario A, B, and D:

The original Townsend scenario A, B, and D is a 1D model. The model is simulated with the 1D governing equation (10). The geometry of the models is illustrated in figure 3. In scenario B the tailings filling rate = 0.02 m/day, and in scenario D the initial void ratio for sand/clay mix = 2.12.
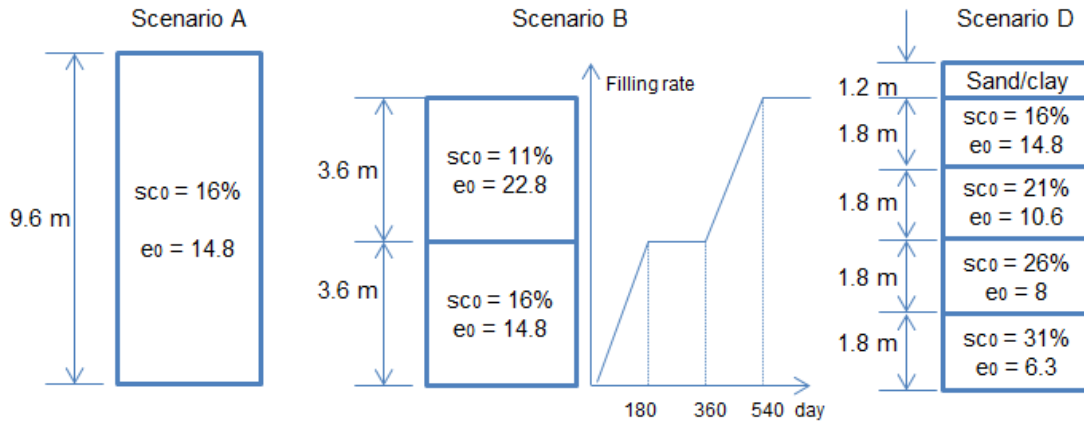
Figure 3. Model geometry for Townsend benchmarking

Power functions were used to represent material behavior in this benchmark. The form of the material relations is defined as the equation (13) and (14) with the parameters $A = 7.72\ kPa$, $B = -0.22$, $C = 2.93E\text{-}12\ m/s$, and $D = 4.56$ for tailings material of scenario A, B and D. The material parameter for sand/clay mixture in scenario D is A = 15.67 kPa, B = -0.24, C = 1.4942E-12 m/s, and D = 4.15.

The upper boundary condition is set to excess pore water pressure $u_e = 0$, and the bottom of the model is considered impermeable.

3.2.2 Model results of 1D Townsend-A, B, and D:

The benchmarks are simulated with 1D model for large strain consolidation (1DLC). The model is setup to simulate for 20 years. The pond height evolution for scenario A, B, and D is shown in figure 4, 5, and 6. The legend of SVSomogyi – 1DLC means the numerical results obtained with the equation (10) of this paper for 1D large-strain consolidation without consideration of sedimentation.
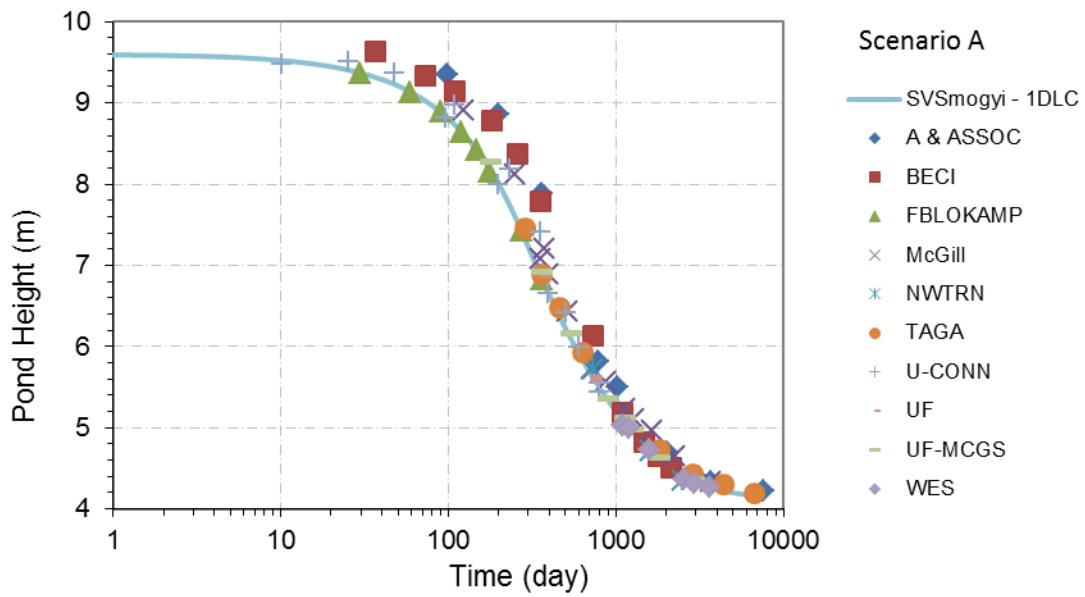
Figure 4. Comparison of predicted pond height of quiescent large strain consolidation for Townsend benchmarking scenario A
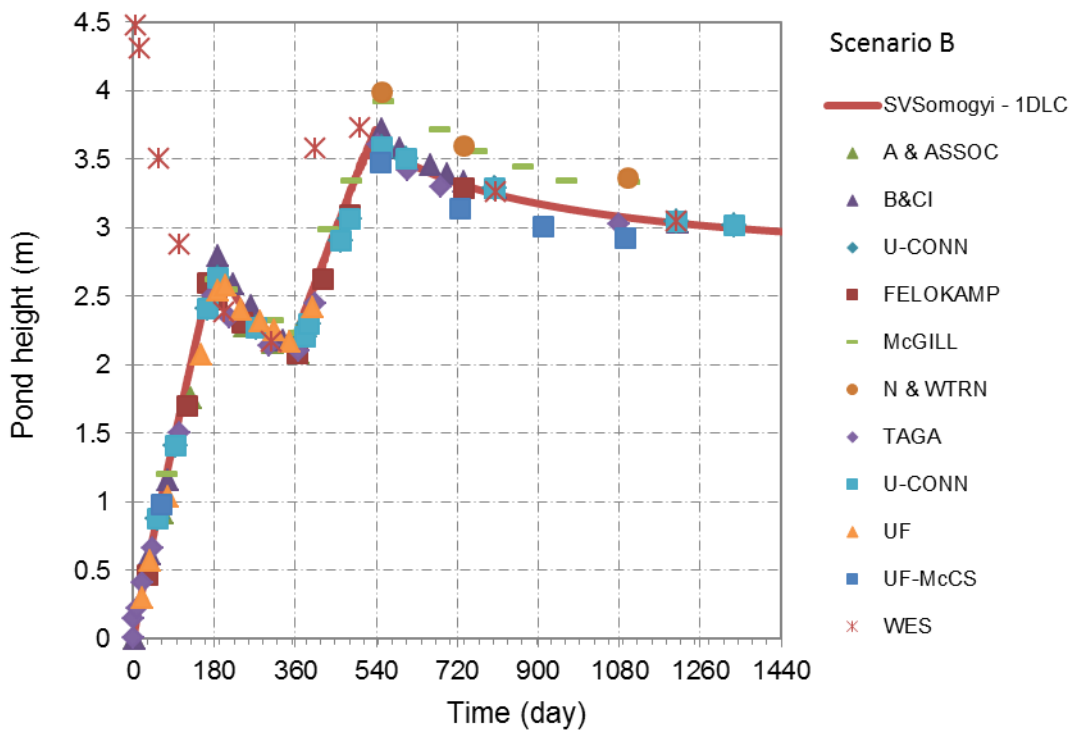

Figure 5. Comparison of predicted pond height with the pond filling and quiescent large strain consolidation for Townsend benchmarking scenario B
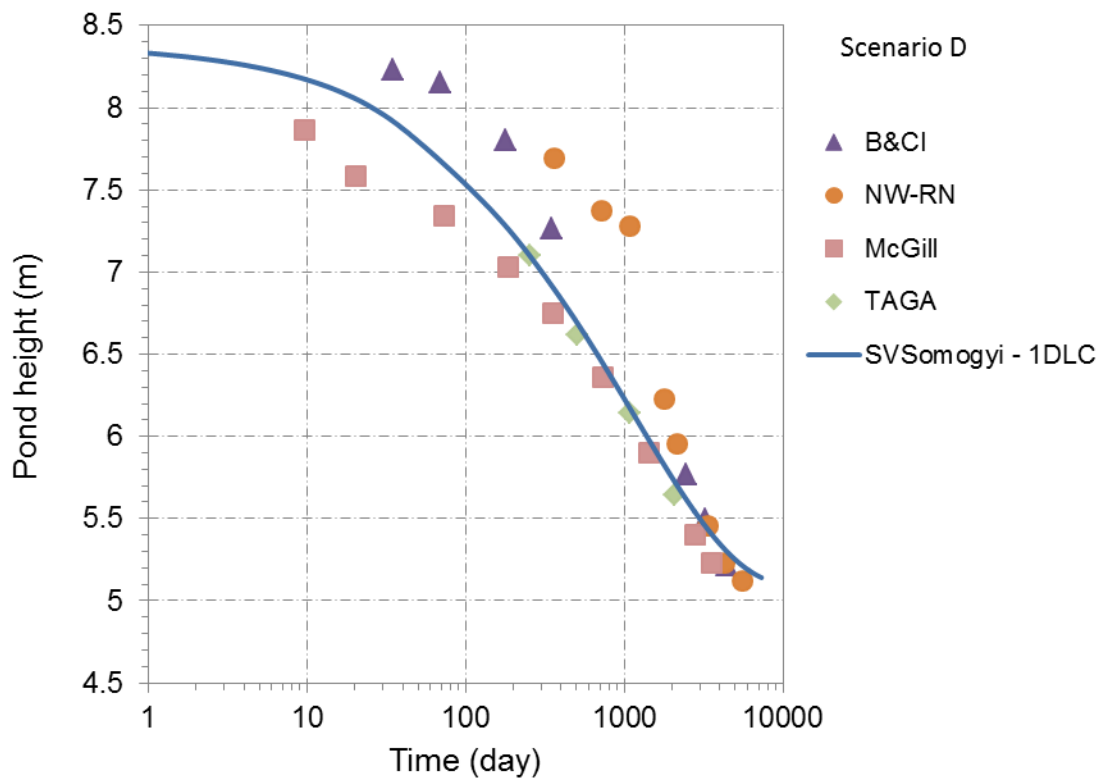
Figure 5. Comparison of the simulated pond height with the multiple layers of quiescent large strain consolidation for Townsend benchmarking scenario D

Figure 6 and 7 present the comparison of profiles of excess pore water pressure and void ratio simulated for Townsend-D benchmarking. It can be seen from figure 4 to 7 that the equation (18) can match the Townsend benchmark reasonable well in the prediction of pond height and profiles of excess pore water pressure and void ratio.
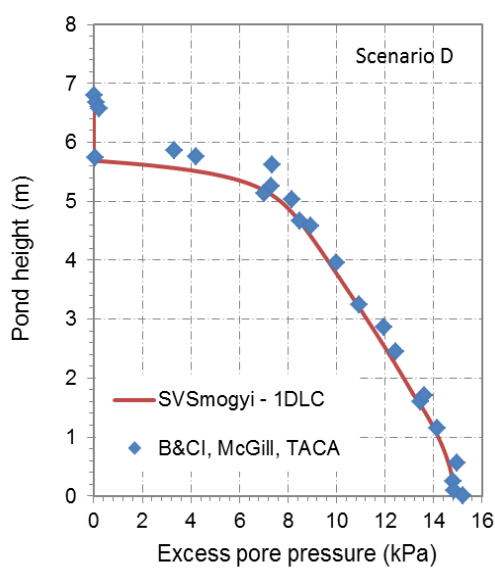

Figure 6. Comparison of profile of excess pore pressure for 1D Large strain consolidation in Townsend-D benchmarking
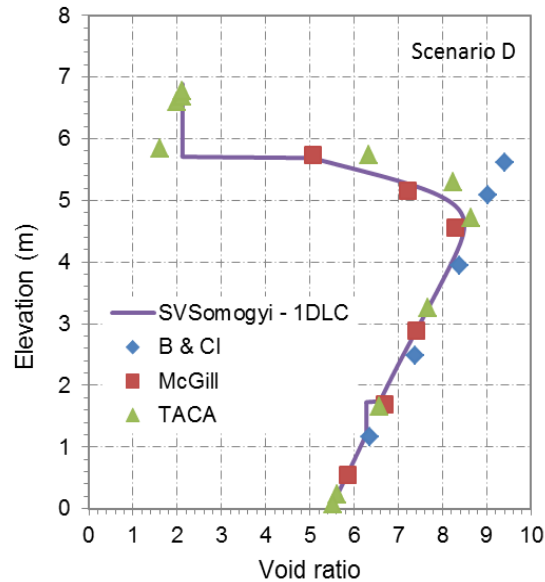
Figure 7. Comparison of profile of void ratio for 1D Large strain consolidation in Townsend-D benchmarking

3.3 *Quasi-2D/3D large-strain consolidation*

There is no significant benchmark available for a 2D/3D model. To verify equation (8), only illustrative models as shown in figure 8 are presented in this paper by applying the same material properties that are used in Townsend-A benchmark. The purpose of these models is to evaluate the difference of the predicted pond height for the 1D/2D/3D models if they have the same values of initial pond height, initial void ratio, and material properties.
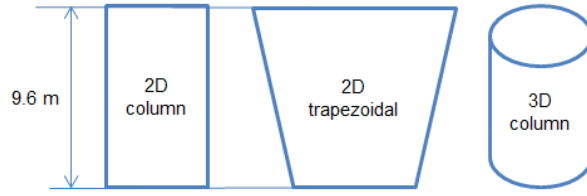

Figure 8. Geometry for the illustrative 2D/3D large-strain consolidation

The solids can freely deform vertically in the lateral side for the models of 2D/3D column, but fixed deformation is used in the slope of 2D trapezoidal model along the bottom and side-walls. Water is considered to be drained at the top, and impermeable at the bottom.

The comparison of the simulated pond height for 1D/2D/3D is illustrated in figure 9. The identical pond height is predicted for the 1D model and the 2D/3D column. There is a slight difference in the predicted value between 1D and 2D trapezoidal model. The difference is likely caused by the fixed deformation setting for the boundary conditions along the slope of 2D trapezoidal model. Figure 8 shows the identical profiles of void ratio obtained for the 1D/2D/3D models, where the elevation is located at central line of 2D/3D model domain. The contour of void ratio is illustrated in figure 9 for these 2D/3D models. Initial mesh is plotted as an indication how much deformation is obtained.

3.4 *The influence factors on sedimentation*

The sedimentation factor is considered through the solid settling velocity v_s in the governing equation (8) and (10) in this paper. The figure 12 and 13 show the effect of settling velocity with the equation (12) and (13) on the pond height in 10 years and profiles of void ratio in 1 year. The Stokes velocity in equation (12) is related to the particle size, which is set to 1 μm in these illustrative models. It can be seen from the figure 11 that the sedimentation has a distinct effect on the settlement of tailings when the void ratio > 6. However, the further investigation is necessary to study the effect of solid settling velocity on the tailings settlement.
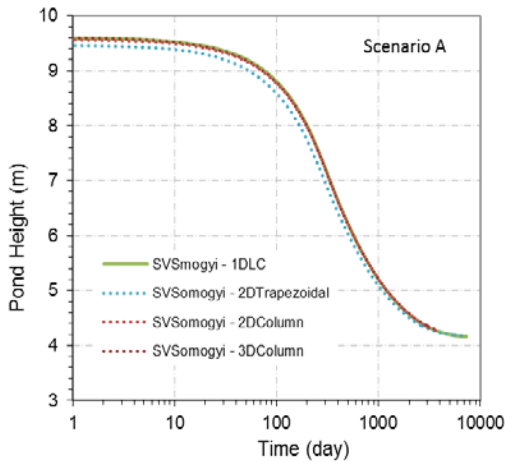

Figure 9. Comparison of pond height simulated by 1D and quasi-2D/3D for the large-strain consolidation with Townsend-A scenario
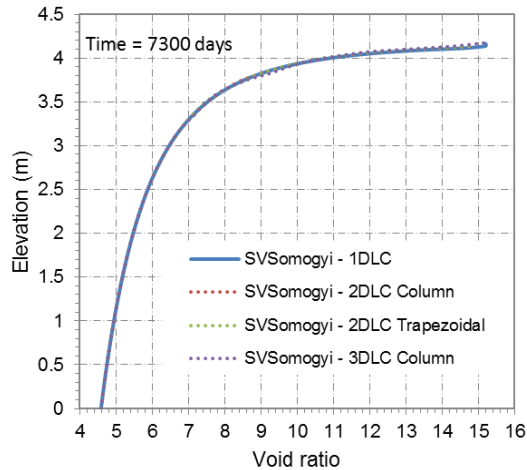

Figure 10. Comparison of profile of void ratio simulated by 1D and quasi-2D/3D for the large-strain consolidation with Townsend-A scenario
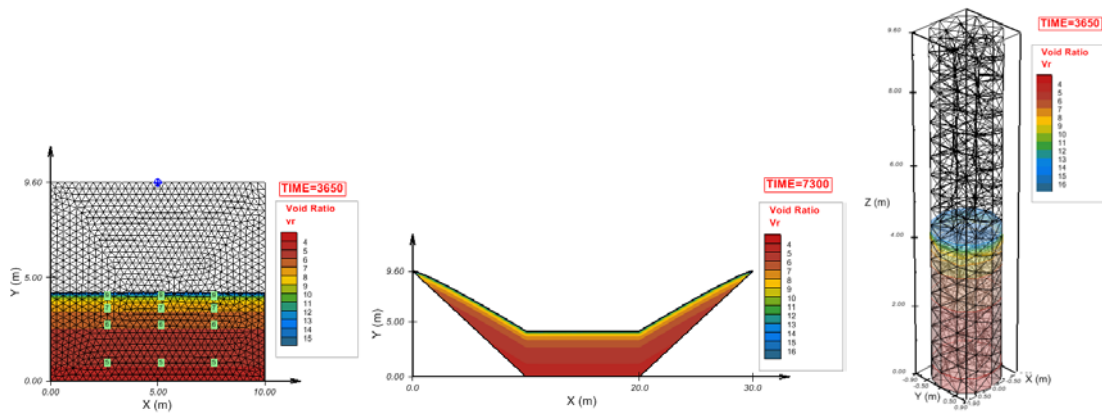
Figure 11. Contours of void ratio for the large-strain consolidation of 2D column, 2D trapezoidal and 3D column model
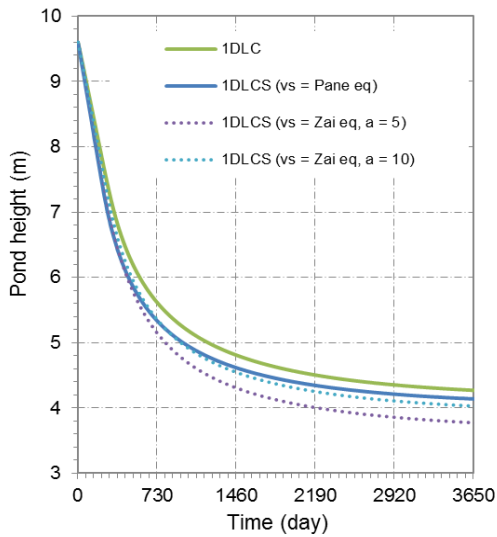

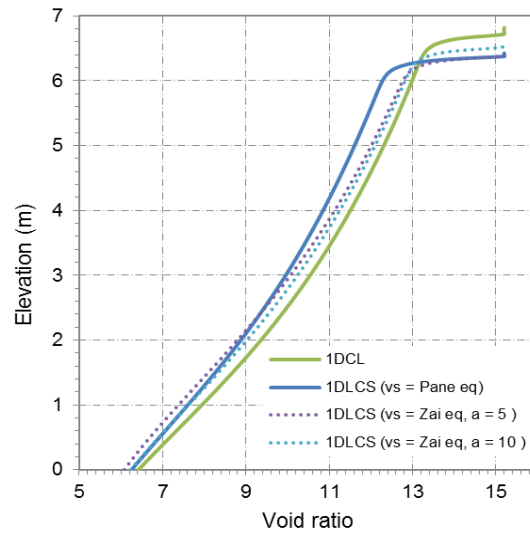Figure 12. Settling velocity effect on the pond height in the 1DLCS

Figure 13. Settling velocity effect on the profiles of void ratio at 1 year in 1DLCS

4 CONCLUSIONS

This paper presented a numerical model formulated in the Lagrangian coordinate to simulate the large-strain consolidation and sedimentation that is similar to the Jeeravipoolvarn equation in quasi-3D case, and to the Somogyi equation in 1D case. SVOffice has implemented the governing equation (8) and (10) as the coupling model of SVFlux and SVSolid software.

Townsend benchmarking scenarios A, B, and D are selected to verify the 1D numerical model and quasi-2D/3D model. The results indicate that the simulation can match well with the Townsend benchmark-A, B, and D in pond height, profiles of void ratio and excess pore water pressure etc. The Townsend benchmark-A is also used to verify the quasi-2D/3D large-strain consolidation and sedimentation. The results obtained from the simulation of quasi-2D/3D model are identical to the values obtained from the 1D model. The sedimentation is included through the solid settling velocity as described by the equation (12) and (13). The Pane & Schiffman equation (13) could be utilized to describe the effect of solids settling on the settlement. Further work will verify the 2D/3D large-strain consolidation and sedimentation with the field data if it is available

5 REFERENCES

Bartholomeeusen, G., Sills, G. & Znidarcic, D. et al. 2002. Sidere: numerical prediction of large-strain consolidation. Geotechnique 52(9): 639-648.

Been, K. 1980. Stress strain behavior of a cohesive soil deposited under water. *PhD thesis,* University of Oxford.

Biot, M.A. 1940. General theory of three-dimensional consolidation. Journal of Applied Physics 12(2): 155-164.

Burger, R. & Wendland, W.L. 2001. Sedimentation and suspension flows: historical perspective and some recent developments. *Journal of Engineering Mathematics* 41:101-1116.

Gibson, R.E, England, G.L. & Hussey, J.L. 1967. Theory of one dimensional consolidation of saturated clay. *Geotechnique* 17: 261-273.

Gibson, R.E, Schiffman, R.L. & Cargill, K.W. 1981. The theory of one dimensional consolidation of saturated clay II. Finite nonlinear consolidation of thick homogeneous layers. *Canadian Geotechnical Jounal* 18: 280-293.

Gustavsson, K. 2003. Mathematical and Numerical Modeling of 1-D and 2-D Consolidation. *PhD thesis*, Royal Institute of Technology, Department of Numerical Analysis and Computer Science.

Jeeravipoolvarn, S. 2010. Geotechnical behavior of in-line thickened oil sands tailings. *PhD thesis*, Edmonton: Faculty of Graduate Studies, University of Alberta.

Lee, K. 1979. Analytical and experimental study of large strain soil consolidation. *PhD thesis*, University of Oxford.

Karl, J.R & Wells, S.A. 1999. Numerical model of sedimentation/thickening with inertial effects. *Journal of Environmental Engineering* 125(9): 792-806.

Kynch, G.J. 1952. A theory of sedimentation. *Trans. Faraday Soc.* 48:166-176.

Masala, S. 1998. Numerical simulation of sedimentation and consolidation of fine tailings. *Master thesis*, Edmoton: Faculty of Graduate Studies, University of Alberta.

McRoberts, E. C. & Nixon, J. F. 1976. A theory of soil sedimentation. *Canadian Geotechnical Jounal* 13: 294 -313.

McVay, M.C., Zuloaga, P.I. & Townsend, F.C. 1988. Reclamation of phosphatic clay waste ponds by 'Capping'. Volume1: Centrifugal model evaluaion of reclamation schemes for phosphatic waste clay ponds. Publication No. 02-030-056. Florida Institute of Phosphate Research.

McVay, M., Townsend, M., & Bloomquist, 1986. Quiescent consolidation of phosphatic waste clays. *Journal Geotechnical Engineering* 112(11): 1033-1049.

O'Neil, S. 2002. Three dimensional bed dynamics for sediment transport modeling. *PhD thesis*. The Ohio State University.

Pane, V. & Schiffman, R.L. 1997. The permeability of clay suspensions. *Geotechnique* 47(2): 273 – 288.

Pane, V. & Schiffman, R.L. 1985. A note on Sedimentation and consolidation. *Getechnique* 35(1): 69-72.

Pollock, G. 1988. Consolidation of oil sand tailings sludge. *Master thesis*. Edmonton: Department of civil and environmental engineering, University of Alberta.

Priestley, D., Fredlund, M. & Zyl, v. 2011. Modeling consolidation of tailings impoundments in one and two dimensions. *Proceedings Tailings and Mine Waste 2011*, Vancouver, BC. November 6 to 9, 2011.

Reichardson. J.F. & Zaki, W.N. 1954. Sedimentation and fluidization. Part1. *Trans. Inst. Chem Eng.* 32: 35 -53.

Qie, Y. & Sego, D.C. 2006. Optimum deposition for sub-aerial tailings disposal: modeling and model validation. *International Journal of Mining, Reclamation and Environment* 30(4): 286-308.

Terzaghi, K. 1943. *Theoretical Soil Mechanics.* New York: J. Wiley and Sons.

Toorman, E.A. 1996. Sedimentation and self-weight consolidation: general unifying theory. *Geotechnique* 46 (1):103-113.

Toorman, E.A. 1999. Sedimentation and self-weight consolidation: constitutive equations and numerical modeling. *Geotechnique* 49(6): 709-726.

Townsend, F.C. & McVay, M.C. 1990. SOA: Large strain consolidation predictions. *Journal of Geotechnical Engineering*, 116(2): 222 – 442.

Yong, R.N. & Elmonayeri, D. 1984. On the stability and settling of suspended solids in settling ponds. Part 11. Diffusion analysis of initial settling of suspended solids. *Canadian Geotechnical Jounal* 21: 644-656

Wells, P.S. 2011. Long term in-situ behavior of oil sands fine tailings in Suncor's Pond 1A. *Proceedings Tailings and Mine Waste 2011*, Vancouver, BC. November 6 to 9, 2011.